From Hospitals to Hurricanes: How APL Is Using Computational Fluid Dynamics to Inform the Future of Public Health and Safety

Ryan A. Darragh, Victoria J. Campbell, Nathaniel S. "Pete" Winstead, Raymond K. Lennon, and Christopher D. Stiles

ABSTRACT

This article discusses how researchers at the Johns Hopkins University Applied Physics Laboratory (APL) are using computational fluid dynamics (CFD) to address public health and safety concerns. CFD, a numerical prediction tool used to simulate fluids, can aid in the design and engineering process by providing insight without the need to physically build or observe a system. Here we present two applications in the public health domain. The first application models and predicts the spread of aerosols in operating rooms in response to the coronavirus disease 2019 (COVID-19) pandemic. The insight derived from this modeling will enable the design of next-generation operating rooms that offer better control of airborne contaminants. The second application focuses on modeling and evaluating the impacts of hurricanes by integrating numerical weather prediction and damage prediction modeling tools. The insight gained from these hurricane simulations enables evaluation of the potential risks and benefits of hurricane modification technology and a greater understanding of the threat of severe storms as a consequence of climate change. From hospitals to hurricanes, the modeling and simulation of fluids can enable insights to inform public health and safety.

INTRODUCTION

Knowledge of fluid motion is essential to engineering design and to improving our understanding of nature. It is critical in the design of aircraft, ships, automobiles, wind turbines, pipes, medical devices, and heating and cooling systems. This knowledge also enables our ability to understand and predict natural phenomena, including weather, forest fires, and supernovae. All these applications depend on the same fundamental laws of nature that together compose the fluid dynamics discipline. It is an exciting field that almost everyone has experience with—most of us have put our hand out the window of a moving car and felt the force of the air push our hand up or down, depending on the angle, or watched as cream mixes with our morning coffee. However, the underlying theory behind these everyday events remains highly complex. In fact, this underlying theory contains "the last unsolved problem of classical physics"—turbulence.[1] Analytic solutions typically exist only in simple flows, such as that of a fluid between two plates. More realistic systems that include complex geometry, turbulence, and additional physics such as heat transfer or chemical and biological reactions must be solved using advanced numerical methods in a process known as computational fluid dynamics (CFD).

In this article, we provide a brief background on CFD, including the governing equations and solution procedure. We discuss how CFD is used to model aerosol spread in operating rooms (ORs) and how these insights are shaping the design of future ORs with better understanding and control of airflow around patients and health care workers (HCWs). We also discuss an internally funded effort that relies on CFD to investigate the effects of modifying sea surface temperature (SST) as a means of mitigating hurricane damage.

BACKGROUND

The first equation governing fluid motion arises from the conservation of mass. It is described with the continuity equation,

$$\frac{\partial \rho}{\partial t} + \frac{\partial \rho u_i}{\partial x_i} = 0,$$

where $\partial/\partial t$ is a time derivative, ρ is the density, $\partial/\partial x_i$ is a gradient, u_i is the velocity, and repeated indices imply summation.[2,3] Next, conservation of momentum is used to obtain the Navier–Stokes equations (NSEs) for incompressible fluid,

$$\frac{\partial u_i}{\partial t} + u_j \frac{\partial u_i}{\partial x_j} = -\frac{1}{\rho}\frac{\partial p}{\partial x_i} + \frac{1}{\rho}\frac{\partial \tau_{ij}}{\partial x_j} + \mathcal{F}_i,$$

where p is the pressure, τ_{ij} is the viscous stress tensor, and $\mathcal{F}_i$ is the volumetric force. It is important to note that the NSEs are inherently multiscale equations, with energy transferring up and down scales through processes such as backscatter and turbulence, making numerical solutions particularly difficult to obtain.[2,3] An additional equation may be created using conservation of energy,

$$\frac{\partial e_0}{\partial t} + u_j \frac{\partial e_0}{\partial x_j} = -\frac{1}{\rho}\frac{\partial u_j p}{\partial x_j} + \frac{1}{\rho}\frac{\partial}{\partial x_j}\left(\kappa \frac{\partial T}{\partial x_j}\right) + \frac{1}{\rho}\frac{\partial u_i \tau_{ij}}{\partial x_j} + u_i \mathcal{F}_i,$$

BOX 1. ORIGINS OF NUMERICAL WEATHER PREDICTION (NWP)

The concept of weather forecasting by numerical methods was first published by Norwegian scientist Villhelm Bjerknes in 1904.[4] Bjerknes proposed a set of equations and a two-phase plan for forecasting. The first phase was a diagnostic step to initialize the atmospheric state from observations. The second phase was a prognostic step to calculate how the atmospheric state changed with time based on the physical laws of motion. Lewis F. Richardson first attempted to forecast the atmosphere from initial conditions while in the field during World War I. While his methods were sound, Richardson incorrectly initialized the atmospheric state, leading to a grossly inaccurate prediction.[5] This discouraged attempts to predict weather for another two decades. Still, Richardson published a book in 1922 titled *Weather Prediction by Numerical Processes*,[6] in which he implemented the prognostic phase of Bjerknes's approach and shared a grand vision for the future of computational NWP, which would prove to be predictive. His visionary idea on how one might go about solving the prognostic step is often quoted: "After so much hard reasoning, may one play with a fantasy?"[6] He describes a large theater resembling a globe (Figure 1) with distributed computers and people performing calculations for individual portions of the globe and portions of equations. A single person in charge would oversee the operation from a tall pillar in the center of the theater. Much like an orchestra conductor, they would ensure all calculations were being done at the same speed. Richardson's vision was far ahead of its time and, remarkably, resembles the concept of modern CFD. NWP is one of the first applications of CFD as we use it today.

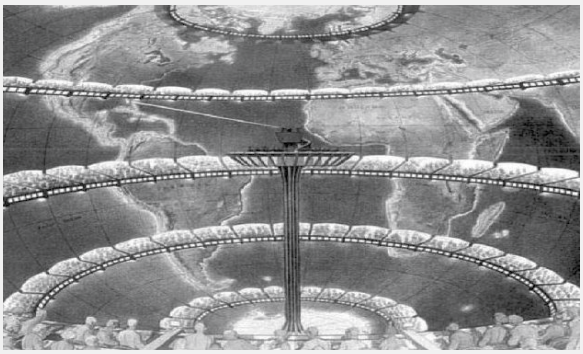

Figure 1. Artist's conception of Richardson's forecast factory. (CC0, via Wikimedia Commons. From J. Lawhead, "Lightning in a bottle," PhD diss., Columbia University, 2014; illustrator F. Schuiten, drawn from P. Edwards, *A Vast Machine: Computer Models, Climate Data, and the Politics of Global Warming*, Cambridge, MA: MIT Press, 2010.)

Richardson's ideas were revisited in the 1940s, owing to the invention of the computer and the growing need for weather forecasting in military operations, particularly during World War II. By using machines instead of humans to make calculations, our forecasting capabilities became faster and more accurate. By the mid-1950s, both the United States and Europe were implementing operational NWP systems, and CFD started to be applied to other fields.[7] From the 1950s to the 1990s, NWP forecasts steadily became more accurate, incorporated increasingly complex model physics, and delivered better spatial and temporal resolution.[5] In the 1990s, NWP forecasting began to incorporate probabilistic forecasting techniques with the advent of ensemble forecasting, which presents a range of future possible forecasts. Ensemble forecasting was an answer to the limitations of deterministic approaches to NWP, accounting for the chaotic behavior of the atmosphere.[8] Both the deterministic and ensemble models are operationally run on supercomputers.[9] The National Weather Service has supercomputers with a combined 42 petaflops of processing power.[10] The ability to computationally and accurately solve these challenging equations for effective predictions has been saving lives for the past century.

where κ is the thermal conductivity, and e_0 is the total energy.[2,3] Finally, an equation of state, such as the ideal gas law, is used to close the system. Additional physics such as heat transfer, chemical reactions, or the impact of local variations in the exchange of energy between the atmosphere and the surface below it can be included by modifying these base equations or including additional equations. All that is left is defining appropriate initial and boundary conditions, and the problem setup is complete.

CFD is critical to many of the analyses APL performs. We leverage CFD when exploring aerodynamics for vehicles in the air and sea, when modeling the sea's impact on sensors in support of field tests, and when modeling biological fluids for medical applications. APL also models particulates, aerosols, and cloud formations for wide-ranging applications, from pollutant tracking to their effects on military systems. As we begin to understand the threats caused by climate change, a number of APL efforts have focused on environmental resilience, informed by CFD and numerical weather prediction (NWP). See Box 1 for a discussion of the origins of NWP.

TRANSMISSION OF DISEASE THROUGH AIR

Background

Several outbreaks of infectious respiratory diseases have occurred over the past two decades, including the severe acute respiratory syndrome (SARS) epidemic from 2002 to 2004,[11] the H1N1 (swine flu) pandemic from 2009 to 2010,[12] the Middle East respiratory syndrome (MERS) outbreak of 2012,[13] and the coronavirus disease 2019 (COVID-19) pandemic.[14] COVID-19 alone severely impacted the global economy, killed millions worldwide, and put frontline HCWs at risk of infection. Health care facilities have already adopted many practices to reduce the spread of disease, such as wearing personal protective equipment,[15] but further work can still be done to better understand and ultimately reduce airborne transmission.

In this article, *airborne transmission* refers to any pathogen that travels through the air either in droplets or on solid particles.[16] Droplets are often produced in processes involving air quickly moving across a liquid surface and creating a shear, which results in a flow disturbance that produces liquid droplets. For example, when someone sneezes, air moves quickly over the mucous in the respiratory tract and droplets are ejected from the nose.[17] The size of these droplets varies, with some being larger than others, and this influences how the droplets and particles move through the air. Larger droplets and particles ($\gtrapprox$100 μm) tend to travel ballistically and quickly fall to the ground, while smaller droplets and particles have a longer settling time and respond more to the surrounding air currents, thus traveling greater distances.[16,18–20] Droplets also tend to evaporate down into droplet nuclei, reducing their size over time and changing how they move through the air.[16,20] This complicates the matter of setting a hard size cutoff between "large" and "small" droplets based on physics alone.[20] However, for modeling purposes we only consider small droplets and particles ($\lesssim$10 μm), termed *aerosols*, in this work.

Preventing disease transmission in operating rooms, and indeed other health care built environments, is essential to ensuring the safety of patients and staff. During surgeries, both patients and HCWs (whom we note should be masked) are potentially exposed to aerosols produced by the staff, surgical equipment, or the patient during procedures that generate aerosols (PGAs). These include any procedure that may cause the patient to generate aerosols (e.g., cutting bone or intubation) that may then travel throughout the room.[21,22] Thus, it is important to understand how these particles might spread during an operation given the airflow in an OR so that precautions can be taken to reduce exposure. While HCWs might be exposed in this manner, we note that frequent occupationally acquired infections due to the airflows described herein are not a common or well-documented problem. Within the OR environment, CFD may also offer insights into the mechanisms contributing to surgical site infections (SSI), specifically pertaining to potential transmission caused by infectious droplets or aerosols depositing at the surgical site. Generally, CFD can be used to provide insight into the spread of aerosols in indoor environments, such as ORs, and can help to explain the factors that influence their movement.

One option for modeling aerosol spread is to directly solve for the motion of each individual particle using Newton's second law and define forces, like drag and gravity, to determine the path a particle follows from its creation until it either collides with an object or leaves the room via an exhaust. By seeding enough particles, we can perform statistical analyses to identify the areas within a room most likely to expose someone to aerosols. We also obtain a time history of a particle, allowing us to discover where the particles move and why.[16,23] However, while particle tracing is a useful technique, it tends to require many trajectories to obtain statistically significant results. As such, this method can be resource intensive and should therefore be used only if necessary (i.e., for large aerosols).

Another approach is to assume that the response time of an aerosol is small relative to the flow timescale (small Stokes number) and consider the particles to be massless. This allows for either simplifying the equation solved to compute trajectories or justifies treating the spread as that of a passive tracer and solving a less computationally expensive concentration transport equation.[16]

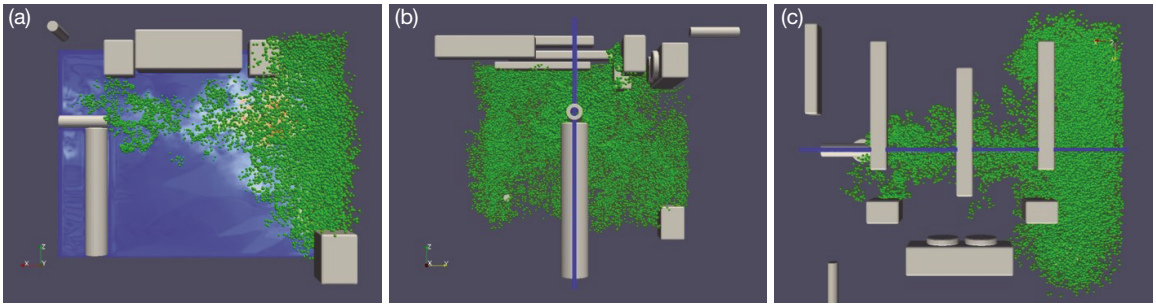

Figure 2. Lattice Boltzmann simulation of a sneeze after 300 s of simulated time. Shown are three different views of the same simulation. The sneeze is generated at the end of the horizontal cylinder on the left-hand side of panel (a). Particles are shown as green spheres, while the gray boxes represent objects in the simulated room that could affect aerosol spread. The background in panel a shows the velocity magnitude, with red, which is mostly obscured by the green particles, indicating faster velocities than blue.

Aerosol Spread Indoors

As an illustration of the first method of particle modeling, the spread of aerosols generated by a sneeze is simulated in an unventilated room using a modified version of the lattice Boltzmann code Sailfish.[24] APL modified this code to include the immersed boundary method to describe solid objects, the cumulant high Reynolds number fluid model, and particle modeling.[25–27] The simulated room was designed to match a chamber at the US Centers for Disease Control and Prevention (CDC) in which an experimental sneeze is generated. We modeled aerosol motion by tracking individual particles subject to Stokes drag and gravity forces and their spread 5 min after generation (shown in Figure 2). Because of the lack of ventilation in the room, particle motion is mostly determined by sneeze-generated airflow, and thus many particles gather near the wall on the opposite side of the room, covering an area from floor to ceiling and wall to wall. Thus, an individual standing opposite the sneezer in this room would be in the presence of many airborne particles. However, this simulation does not account for all factors in the rooms people commonly occupy, including different ventilation systems and the location of flow-disrupting objects that may alter the aerosol distribution throughout the room.

Aerosol Spread in ORs

The infectious risks of aerosols in ORs are currently mitigated using a combination of infection prevention and control (IPC) procedures and protocols, correct

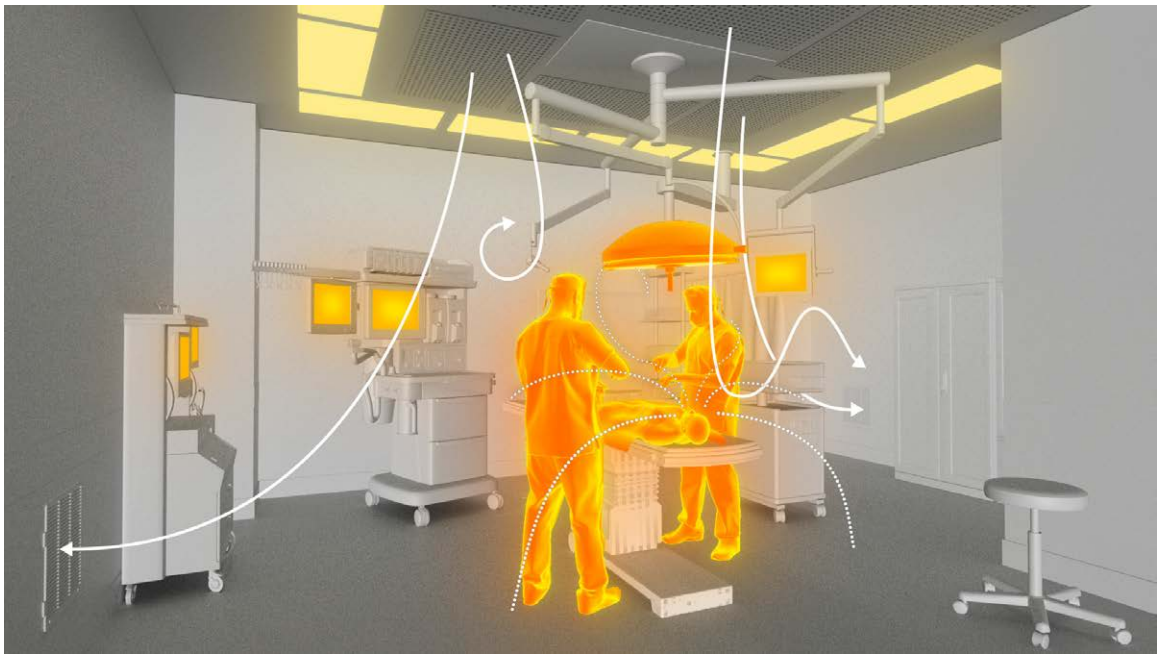

Figure 3. The main drivers of aerosol movement in an OR include the heating, ventilation, and air conditioning (HVAC) system; buoyancy induced by people and heated equipment; and the PGA itself. Solid lines denote potential streamlines originating from the above HVAC supply, and dotted lines indicate several potential aerosol trajectories. Heated bodies are colored orange.

use of personal protective equipment, and often a ventilation system built specifically for the OR environment.[15] The ventilation used often employs a unidirectional airflow supply system designed to reduce the occurrence of SSIs caused by particles landing in the surgical wound.[28] This system is designed to wash aerosols away from the surgical site by directing slow, cool air down over the surgical table.[29] Because the air is slow to avoid any enhanced mixing due to turbulence, the ventilation system is called a laminar airflow system (LAF). However, flow obstructions like surgical lights and other equipment are often present in the surgical zone, disrupting the flow and altering the path of aerosols.[30–32] These obstructions may trap some aerosols in their wake, while others may leave the surgical zone but linger in the room or be carried up to the ceiling and back over to the supply jet where they then may become entrained and reenter the surgical zone.

Medical equipment and people also release heat, causing the air to warm up, become less dense, and rise because of the buoyant forces in a thermal plume.[28] This often results in unsteady flow and further complicates efforts to predict and control aerosol movement. Another potentially large driver of airflow is the movement of people and equipment within the OR. Cooling fans required to run medical equipment disturb the flow by ejecting jets of air, and people walking both push the air in front of them and leave behind a wake. This movement has an overall effect of disrupting the surrounding flow, a particularly important fact when entering or leaving the LAF region since aerosols could be brought into the surgical zone.[33] The door to the OR is also opened frequently, removing the pressure difference between the OR and hallway and potentially allowing aerosols to enter the OR.[28] Figure 3 summarizes these major influences on aerosol motion in an OR, including a PGA at the head of the patient.

These effects can all be investigated using COMSOL Multiphysics to simulate 3-D airflow in an OR.[34] Figure 4a shows the geometry of an OR including a

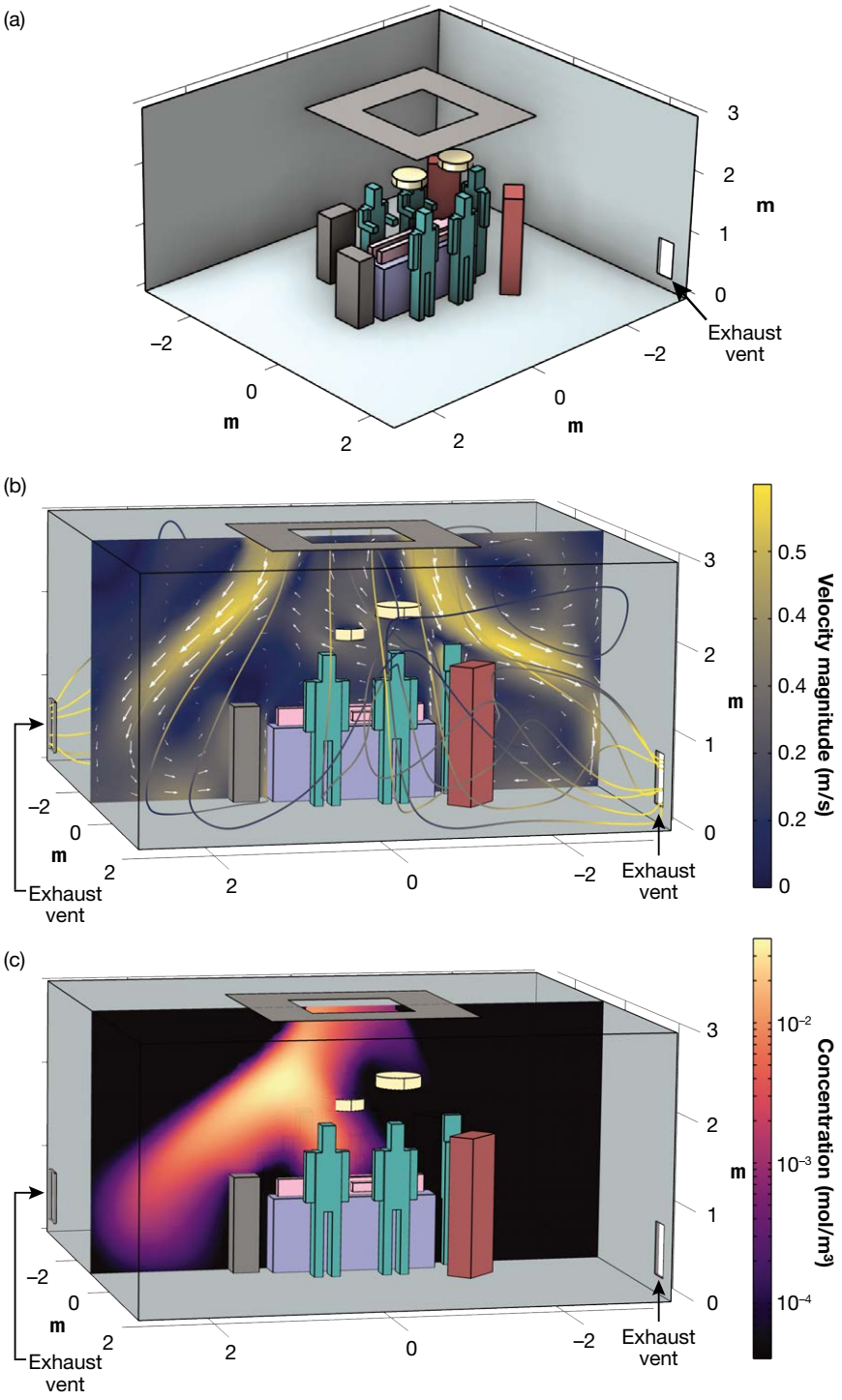

Figure 4. Airflow and aerosol spread in an OR. (a) Geometry of 3-D OR simulations. Surgical lights are shown in yellow, heated equipment in red, unheated equipment in gray, HCWs in dark cyan, and the patient and surgical table in light cyan. (b) The velocity magnitude and streamlines at a single instant in time. (c) The concentration 15 s after the start of a 5-s PGA.

surgical table with LAF ventilation blowing down and being obstructed by surgical lights. The LAF itself is also obstructed at the ceiling, resulting in no air entering the room in the center of the supply diffuser grid. Several HCWs are standing around the patient, along with two pieces of heated and unheated medical equipment. Heat emitted by the people and equipment induce buoyancy, causing the flow to become unsteady and resulting in a time-dependent flow. The NSEs, with the standard k-ϵ turbulence model, are solved along with a coupled energy equation to account for buoyancy. Flow enters from the LAF diffuser on the ceiling at 0.43 m/s and 19°C and exits through one of two exhausts located in opposite corners of the room. The patient, HCWs, two surgical lights, and two taller pieces of medical equipment are all heated. The room is divided into about three million elements in which the governing equations are solved using the finite element method. Overall, this simulation took roughly 3 days to complete while running on two Intel Xeon CPU E5-2650 v4 at 2.20 GHz.

Of particular interest is the fluid behavior above the table near the patient and HCWs. Figure 4b shows a lower-velocity magnitude above the patient, relative to the inlet velocity, due to the obstruction at the ceiling. Obstructions like this are common in ORs and serve as a mounting point for equipment such as surgical lights, as shown in Figure 3. Higher-speed air is pushed off to the sides of the surgical zone, which may still help to protect the patient from an external aerosol source by deflecting aerosols originating from outside the surgical zone. However, aerosols generated within the surgical zone of this OR may not be washed away as quickly because of the obstruction at the ceiling and the placement of the two surgical lights. Flow can also be seen traveling upward beneath the obstructions and near the heated bodies. Several streamlines originating from the HVAC supply are found to be spiral-shaped behind the two closest HCWs in Figure 2b; this extended path indicates a longer residence time of aerosols in the room. This OR could potentially be modified to reduce the trapping of aerosols within the surgical zone; for example, adding exhausts near the ceiling or obstructing less of the HVAC supply may drastically change the airflow.

Figure 4c shows the concentration field of aerosols 15 s after the start of a 5-s PGA located on the stomach of the patient. Most of the concentration remains in the surgical zone, with a large portion at and above the head height of the surrounding HCWs. In particular, the two HCWs near the feet of the patient reside in a region of greater concentration at this point in time. Eventually the concentration will decrease as aerosols leave the surgical zone and eventually the room.

Lagrangian methods provide another view into the behavior of aerosol particles. Figure 5 shows a 3-D OR with exhausts on opposite corners, a patient lying on a surgical table in the center, a surgical light above, and a surgeon standing beside the bed. Flow enters from the LAF supply on the ceiling and particles are released in a grid immediately above the patient's body. The path lines of these particles are then tracked throughout the room. While buoyant effects are not included in this simulation, particles are still found to travel upward in the wake of the surgical light and as they approach the walls of the OR along the floor. Aerosols directed up by the wall and back over to the surgical zone may become entrained into the jet and directed down over the patient and surgeon.

Simulations of indoor airflow and contaminant spread within ORs allow for insight into the flow near the patient, which is typically difficult to measure experimentally during an operation, but the same conditions can be represented and simulated using CFD. New OR designs and room configurations can also be tested quickly, cheaply, and without any burden to patients or HCWs in order to identify new layouts that can then be incorporated into current health care operations or built into the next generation of ORs. Outside of health care settings, CFD simulations of indoor airflow provide a similar benefit for any location that may be at risk of an airborne contaminant—for example, the spread of contaminants in a manufacturing facility or a dangerous substance released into a building by an adversary.

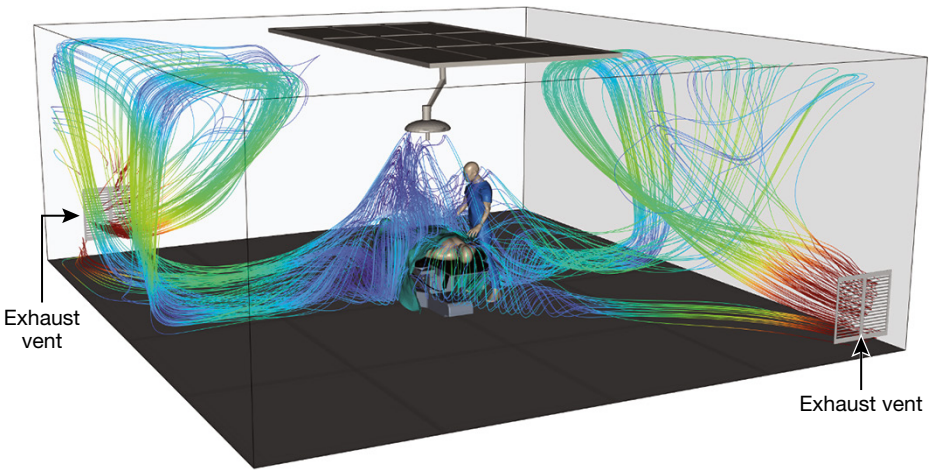

Figure 5. Particle path lines in a 3-D OR. Trajectories are colored by velocity, with blue being slower than red. Simplified geometries were used to represent the surgeon, patient, bed, and surgical light in the simulation; detailed versions are included for graphical effect.

NWP FOR HURRICANE ANALYSIS

Overview

Hurricanes represent a significant threat to coastal areas across the globe. In the United States alone, they incur annual costs exceeding $50 billion[35] and have devastating humanitarian impacts worldwide. Research suggests that hurricanes may grow more intense in a warming world, increasing the threat to coastal populations.[36] To address this threat, researchers have reexamined an old question: Can a hurricane be modified in some way to lessen its severity? Recent improvements in reduced forecast errors and earlier available warnings have strengthened the case for weather modification as a defense against increasingly severe extreme weather due to a changing climate. With expertise in systems engineering and NWP, APL can evaluate the feasibility of proposed concepts by assessing the impact. The independent research and development (IRAD) effort described below demonstrates the unique assessment capabilities of NWP.

This research aims to use CFD in the form of NWP to assess physics-based impact measures for evaluating proposed technologies for weather modification. This involves modifying the environment in the path of a potential tropical cyclone, and then simulating the impact on a particular hurricane with NWP. Storm characteristics (such as maximum wind speed, minimum central pressure, and rainfall) are generated both for unmodified and modified storm environments. We assess the physical differences between the various simulated storms using FEMA's HAZUS-MH[37] to identify differences in expected storm damage. This modeling pipeline is presented through analysis performed on Hurricane Michael, a category 5 storm that made landfall in Florida in October 2018.

Background

The tool most widely used at APL for NWP is the Weather Research and Forecasting Model (WRF) from the Mesoscale and Microscale Meteorology Laboratory of the National Center for Atmospheric Research.[38] The core Advanced Research WRF (ARW) Solver solves the fully compressible non-hydrostatic NSEs for modeling the atmosphere. The WRF-ARW also assimilates real data initializations to provide more accurate predictions. With this tool, we can model CFD weather events using APL's high-performance computing resources on scales of tens of meters all the way up to thousands of kilometers.

The impact of improvements to NWP over the last century cannot be overstated; NWP is one of modern science's greatest successes. Modern weather forecasts are astonishingly accurate. Specifically for hurricanes, today's 72-hour predictions are more accurate than 24-hour forecasts were 40 years ago.[39] Forecasts that are both earlier and more accurate allow for more time to evacuate and respond to the disaster, saving lives and property. This advancement opens the door to previously unimaginable hurricane modification technology.

Weather modification like this, particularly applied to hurricanes, has a long and controversial history (see for example, Project STORMFURY[40]). Despite past controversy, experts have started to reconsider modification as an option to mitigate severe weather events, especially as they become more frequent and catastrophic because of climate change. Examples of this interest include the publication of feasibility studies[41–43] proposing environmental modifications ahead of a hurricane to impact its development. The most promising of these techniques involves cooling the SST to reduce the heat flux into the storm, which is a well-known contributor to hurricane intensity.[44] The technique of artificial upwelling is well known in the geoengineering community and has taken many forms, from aquaculture to carbon sequestration to energy production.[45] In a study funded by the Department of Homeland Security, researchers analytically assessed potential cost savings for hurricane defenses, specifically evaluating the potential cost savings of using wind-wave pumps to modify SST off the Florida coast.[41] The lead author of this study concluded in her dissertation that if it could be feasibly implemented, this modification could reduce net wind losses from an intense storm.[41] However, the study found modification problematic because of uncertainty of success and concerns about the public's perception of modification generally.

The scientific community recognizes the need for hurricanes in various ecosystems and is not proposing or supporting an effort to stop all hurricanes. Instead, the hope is that modifications might reduce the severity of a particular storm, with the "success" metric being damage reduction. Because damage scales as the square of wind speed, researchers hope that small changes in a hurricane's structure and strength during formation might have a significant impact on the storm's strength at landfall.

While the advances outlined above suggest the need to revisit hurricane modification, the field lacks a systematic approach to evaluate potential modification technologies in an objective, science-based way. Fortunately, high-resolution NWP codes such as WRF have the requisite physics to simulate the impact of many potential modification technologies in a rigorous, controlled manner. In this modeling effort, we are working to develop an end-to-end, physics-based system to evaluate the feasibility and impact of modifying the environment before a hurricane's arrival.

Hurricane Michael NWP Modeling Pipeline

We used Hurricane Michael to illustrate how a modeling pipeline might look operationally. Hurricane Michael formed in early October 2018 in the Gulf

of Mexico. It rapidly intensified over 2 days, reaching an ultimate intensity of 140 knots (category 5 on the Safir–Simpson Scale) as it made landfall near Mexico Beach and Tyndall Air Force Base in Florida on October 10, 2018. Michael is an excellent candidate for case-study analysis for several reasons. First, the storm was exceptionally well forecast. Operational products highlighted the possibility of a strong hurricane 5 days before it formed, and track errors were less than the 5-year average track errors.[46] Therefore, meteorologists were able to predict Hurricane Michael's arrival well in advance of its formation and arrival.[46] Second, Michael occurred in a self-contained ocean basin. This simplified the atmospheric modeling component of this storm. Finally, Michael was a very powerful storm that directly impacted a coastal Department of Defense facility (Tyndall Air Force Base). Ultimately, Michael was responsible for at least $25 billion in damage.[46] For these reasons, Michael is an excellent test case for illustrating the modeling pipeline described here.

We used the WRF-ARW to forensically reconstruct Hurricane Michael and to test the effectiveness of weather modification. In recreating this storm as a case study, we developed a modeling pipeline (Figure 6) around NWP to quantify the impact that environmental modifications might have on a storm's eventual damage. The simulations run in this study were based on modifying the skin temperature of the lower initial boundary condition to replicate the effects of proposed weather modification concepts of using deepwater upwelling to reduce SST in the path of a hurricane.[47] It should be noted here that to properly account for the impact of any upwelling, a fully coupled ocean/atmosphere simulation is needed to account for the very complex interactions at the ocean/atmosphere interface. The current modeling approach is not accounting for these processes and is therefore likely to overestimate any impact from SST modifications. However, the current modeling chain does provide self-consistent comparisons between a control simulation with no modification and the relative impact of SST modifications for various configurations of deployed pumps.

Figure 6 shows the current modeling pipeline used for the initial studies on Michael. The first step in this modeling pipeline is our MATLAB model of upwelling technology for SST reduction plot, which models the reduction in SST from using pumps to upwell cooler water from ocean depths.[48] The user inputs the pump dimensions, position, and run time, and a net SST cooling rate is calculated based on an observed ocean profile. With this code, the user can determine achievable SST cooling as a function of time. The considered pump type is a wave-powered pump, consisting of a surface buoy connected to a long cylindrical pipe with radius r that extends underwater. The pipe has a one-way valve at the bottom that opens when the buoy descends in a wave trough and closes at the next wave peak. Inertial forces associated with wave motion impel cooler water into the pipe when the valve is open and propagate it along the pipe length. After repeated cycles, the cooler water eventually makes it to the top of the pipe where it expels the upwelled water into shallow warm water. This model is based on a theoretical analysis of wave-powered pumps[49] and a published framework consistent with this IRAD effort.[48] It is also based on a specific design of the wave-powered pump.[45,50] The information on sea state is taken from a nearby buoy through the National Data Buoy Center (Station 42039),[51] and temperature profile information is pulled from the appropriate Argo float.[52] This part of the modeling chain can be deployed anywhere that wave and vertical ocean temperature data can be obtained.

Once we have estimated a "modified" skin temperature field, we run WRF-ARW with in a tropical configuration on both unmodified (control) and modified SST fields based on various pump configurations. Postprocessing the WRF outputs allows us to compare impacts on track, time and location of landfall, minimum central pressure over time, maximum wind speed over time, accumulated rainfall over time, and integrated kinetic energy (IKE)[53] over time. The results from each of these simulations can then be input into HAZUS-MH where damage cost functions are applied to the meteorological parameters. This gives estimates of wind damage and storm surge flooding using HAZUS-MH and provides an aggregate direct economic loss value.

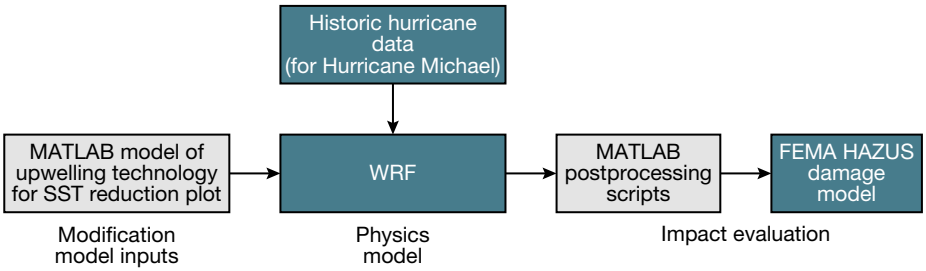

Figure 6. Modeling pipeline used to assess the impact of hurricane modifications. The blue boxes indicate commercial off-the-shelf data or analysis software leveraged within the pipeline. The gray boxes indicate APL-developed analysis tools.

Results and Discussion

The forensic recreation of Hurricane Michael serves as the control study for the modification impact assessment. Several WRF simulations were performed, each of which varied modification strategies. In every set

of simulations, a control was generated that represented the "unmodified" storm. In the modification cases, the pump model described above was used to generate modified SST skin temperature fields. WRF was then run using the modified fields. These simulations are then compared against the control simulation to determine the relative impact of the modifications.

As an illustration of this process, results from the control simulation are shown below. In this case, WRF was run with a grid spacing slightly less than 1 km (666.67 m). Panels (a) and (b) in Figure 7 show the comparison of the models simulated maximum wind speed and minimum sea level pressure with the official intensity metrics reported in the National Hurricane Center (NHC) Storm Summary for Michael. Panels c and d show the comparison of the model's simulated IKE with the thresholds of tropical storm force winds and category 3 wind speeds on the Saffir–Simpson scale.

To generate the modified runs, the pump model was configured based on a 300,000-pump case where the pumps were deployed in a rectangle along the path of the storm. Because these pumps require significant depth to work, the box is constrained to lie off the continental shelf in deep water. So that the size of the box could be

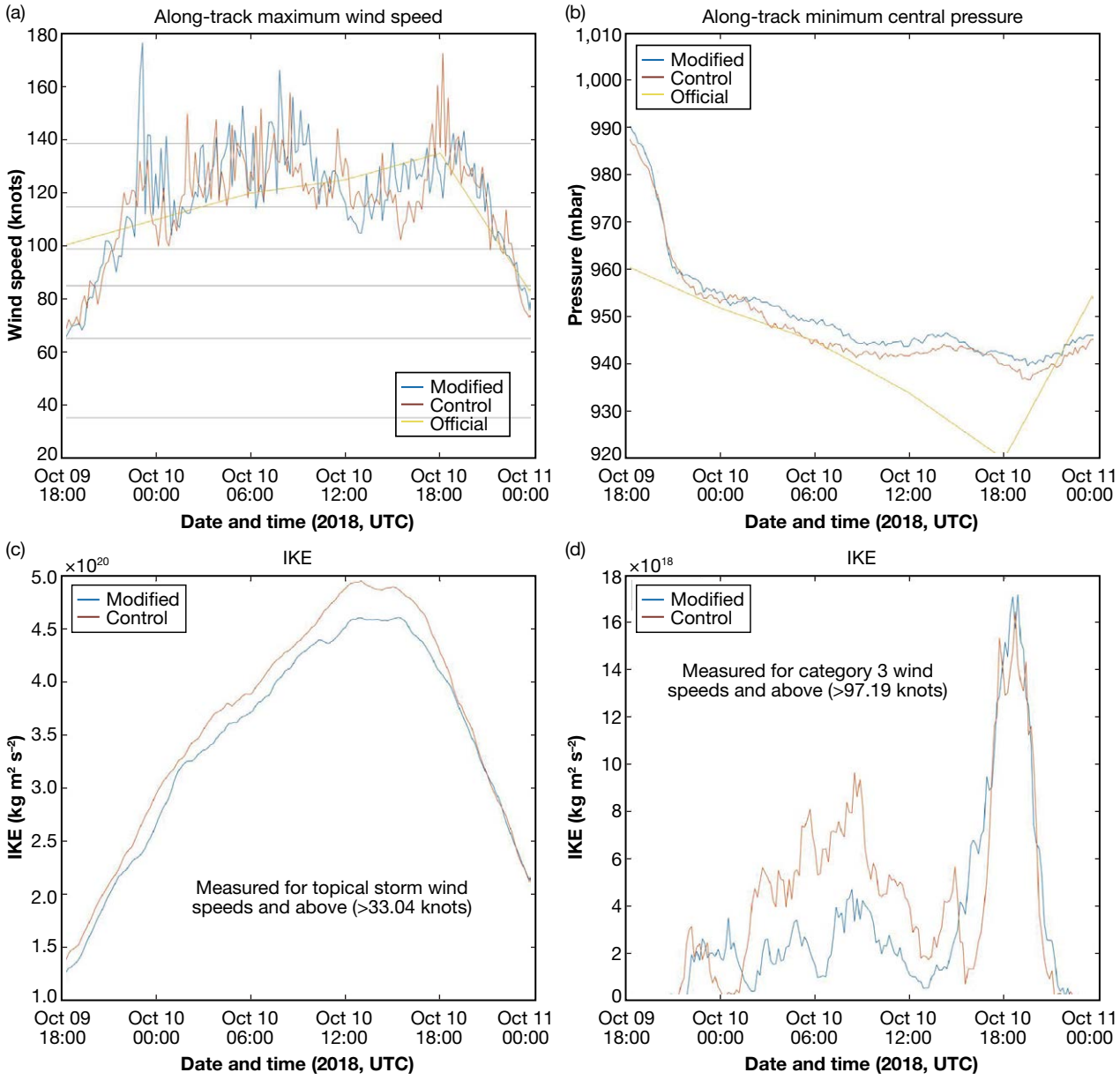

Figure 7. The physical measures of the modeled control and modified Hurricane Michael as the storm approached landfall on October 10, 2018. (a) Maximum wind speed (knots) 10 m above the ground compared with the official statistics published in the NHC storm summary. (b) Minimum central pressure (mbar) compared with the official statistics published in the NHC storm summary. (c and d) The time-varying IKE of the storm compared between the models with thresholds of 33.04 knots and 97.19 knots, respectively.

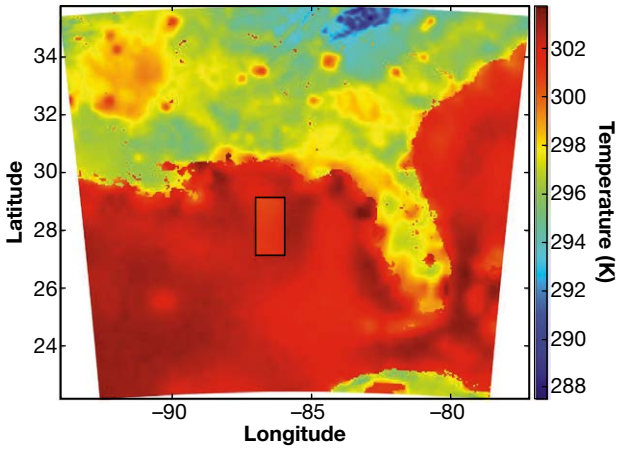

Figure 8. Modified SST field based on the 300,000-pump configuration resulting in a ~1.5 K change in temperature. The modified area is the rectangle in the Central Gulf of Mexico.

optimized for this illustration, it was presumed ahead of time that the forecast track was perfectly known so that the time that the eyewall (and eye) of the storm would cross over the modified area was maximized.

Figure 8 shows the results from the pump model for this configuration. For a 300,000-pump configuration where the pumps are active when the wave field ahead of Michael reaches the threshold for pump activation, ~1.5 K of SST cooling is achievable. The 300,000-pump value was derived from Klima et al.,[41] where the different regions presented would require 200,000 to 400,000 pumps based on the 333-m spacing provided. This study did not address the mechanics of deploying that many pumps over a short time; obviously, the magnitude of this deployment presents logistical challenges.

Table 1. Resulting damage analysis from HAZUS-MH for both the control WRF run and the modified WRF run

	Total Estimated Economic Loss (Millions USD)		
	From Floods	From High Winds	Total
Control	510	26,411	26,921
Modified	284	21,996	22,280

With respect to the impact of the modification, Figure 7 (a and b) shows the maximum wind speed and minimum sea level pressure differences due to the modification. A more in-depth analysis of the spatial structural changes to the storm is ongoing, but wind speed and sea level pressure are the two typical metrics used when reporting hurricane strength. Interestingly, the modifications to the wind speed are quite subtle. The additional metric of IKE has been shown to be a better indicator of damage,[53] as shown in Figure 7 (c and d).

HAZUS-MH provides observation data inputs for the historic storm Hurricane Michael to directly compare the damage assessment with our NWP hurricane model. Figure 9 shows the results from running HAZUS-MH on the control and the modified storm. The track fluctuations are likely the result of pressure fluctuations within the eye itself as the storm strengthened rapidly. Table 1 shows the aggregate economic damage estimates from HAZUS-MH for bay and gulf counties in Florida. Although these values are not validated, the relative comparison implies a 17% difference in potential storm damage. A full damage analysis incorporating all affected counties was not attempted.

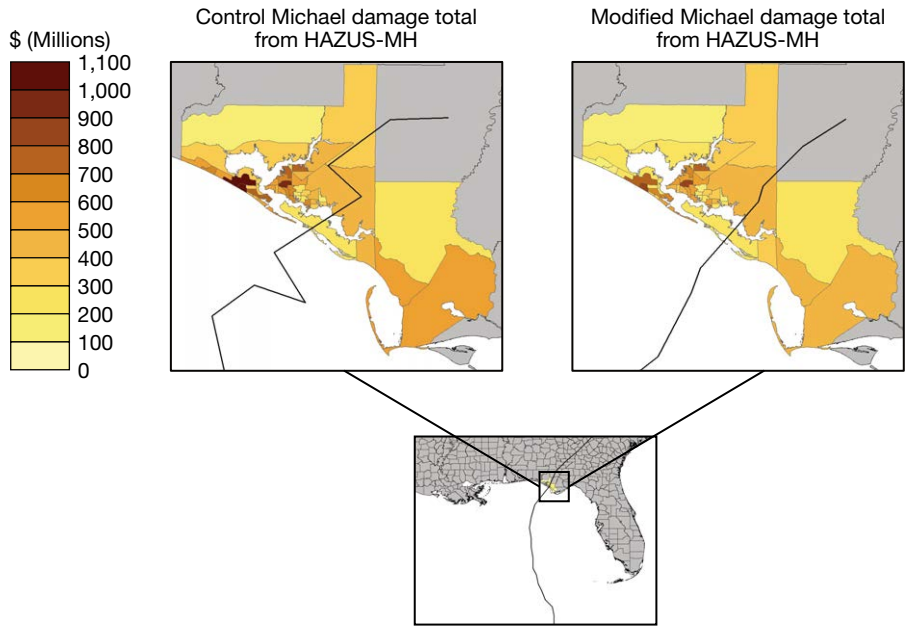

Figure 9. Damage analysis from HAZUS-MH for both the control WRF run and the modified WRF run. The black line represents the storm track as defined by the minimum central pressure. The damage key is consistent for both model results.

These results demonstrate the value of the modeling pipeline and in representing impact through predicted damage instead of common physical terms. Feeding NWP into damage assessment tools can provide new opportunities for insights and ways of considering the severity of a storm. Although the Saffir–Simpson scale is the most common way to communicate the severity of a storm as a category based on wind speed, it is neither intuitive nor directly

related to the potential cost of damages. When quantifying the impact of a singular storm or considering if a modification technology would be worth the investment, we need to look beyond just physical understanding and communicate that impact in terms of damage.

CONCLUSION

Fluid modeling is essential to many engineering systems and to improving our understanding of natural phenomena. This article focused on two CFD applications to public health and safety and the insights gained in their modeling. In the first, we simulated the indoor airflow in an OR, revealing the potential for aerosols to linger in the wake of flow obstructions and to move vertically in and out of the surgical zone. Additional simulations like those described in this article will help to better inform patient and HCW exposure to aerosols in ORs and allow for rapid testing of different room configurations, object and staff placement, and ventilation strategies.

For the second application, related to weather modification—specifically exploring whether modifying SST affects the potential damage caused by a hurricane—we found that the physical measures of a storm's severity, while informative, do not capture the impact of a hurricane. When assessing the viability of hurricane modification technologies, the impact must be quantified—and it can be with the modeling pipeline presented. While the scales of these two applications are very different, both are modeled using CFD at APL. As our computing hardware continues to advance, CFD will be able to provide more accurate and refined fluid simulations and continue to expand engineering design capabilities and our understanding of the natural world.

ACKNOWLEDGMENTS: We gratefully acknowledge Sunny Sharma (APL) and Ben Schmachtenberger (APL) for their software development and analysis support for the hurricane research, as well as funding support from APL's Research and Exploratory Development Mission Area. We gratefully acknowledge the US Centers for Disease Control and Prevention (CDC) for funding part of this work. Part of this material is based on work supported by the Naval Sea Systems Command (NAVSEA) under Contract No. N00024-13-D-6400, Task Order NH076. Any opinions, findings, and conclusions or recommendations expressed in this material are those of the author(s) and do not necessarily reflect the views of NAVSEA or the CDC.

REFERENCES

[1]G. Falkovich and K. R. Sreenivasan, "Lessons from hydrodynamic turbulence," *Phys. Today*, vol. 59, no. 4, p. 43, Apr. 2006, https://doi.org/10.1063/1.2207037.

[2]I. M. Cohen, D. R. Dowling, and P. K. Kundu, *Fluid Mechanics*, 5th ed. Waltham, MA, USA: Academic Press, 2012.

[3]S. B. Pope, *Turbulent Flows*, 1st ed. Cambridge, United Kingdom: Cambridge University Press, 2001.

[4]V. Bjerknes, "The problem of weather prediction, as seen from the standpoints of mechanics and physics," *Meteorologische Zeitschrift*, 1904.

[5]F. G. Shuman, "History of numerical weather prediction at the national meteorological center," *Weather and Forecasting*, vol. 4, no. 3, pp. 286–296, Sep. 1989, https://doi.org/10.1175/1520-0434(1989)004<0286:HONWPA>2.0.CO;2.

[6]L. F. Richardson, *Weather Prediction by Numerical Process*, 2nd ed. Cambridge, United Kingdom: Cambridge University Press, 2007.

[7]P. Lynch, "The origins of computer weather prediction and climate modeling," *J. Comput. Phys.*, vol. 227, no. 4, pp. 3431–3444, Mar. 2007, https://doi.org/10.1016/j.jcp.2007.02.034.

[8]E. N. Lorenz, "Deterministic nonperiodic flow," *J. Atmospheric Sci.*, vol. 20, no. 2, pp. 130–141, Mar, 1963, https://doi.org/10.1175/1520-0469(1963)020<0130:DNF>2.0.CO;2.

[9]T. Gneiting and A. E. Raftery, "Weather forecasting with ensemble methods," *Science*, vol. 310, no. 5746, pp. 248–249, Oct. 2005, https://doi.org/10.1126/science.1115255.

[10]S. Buchanan, "U.S. supercomputers for weather and climate forecasts get major bump," press release, National Oceanic and Atmospheric Administration (NOAA), Jun. 28, 2022, https://www.noaa.gov/news-release/us-supercomputers-for-weather-and-climate-forecasts-get-major-bump.

[11]Centers for Disease Control and Prevention, "Severe Acute Respiratory Syndrome (SARS)," cdc.gov. https://www.cdc.gov/sars/index.html (accessed Nov. 1, 2021).

[12]Centers for Disease Control and Prevention, "2009 H1N1 Pandemic Timeline," cdc.gov. https://www.cdc.gov/flu/pandemic-resources/2009-pandemic-timeline.html (accessed Nov. 1, 2021).

[13]Centers for Disease Control and Prevention, "Middle East Respiratory Syndrome (MERS)," cdc.gov. https://www.cdc.gov/coronavirus/mers/about/transmission.html (accessed Nov. 1, 2021).

[14]Centers for Disease Control and Prevention, "COVID-19," cdc.gov. https://www.cdc.gov/coronavirus/2019-ncov/ (accessed Nov. 1, 2021).

[15]R. K. Bali. "Operating Room protocols and infection control," in *Oraland Maxillofacial Surgery for the Clinician*. Singapore: Springer, 2021, pp. 173–194.

[16]V. Vuorinen, M. Aarnio, M. Alava, V. Alopaeus, N. Atanasova, et al., "Modelling aerosol transport and virus exposure with numerical simulations in relation to SARS-CoV-2 transmission by inhalation indoors," *Safety Sci.*, vol. 130, art. 104866, Oct. 2020, https://doi.org/10.1016/j.ssci.2020.104866.

[17]J. Fiegel, R. Clarke, and D. A. Edwards, "Airborne infectious disease and the suppression of pulmonary bioaerosols," *Drug Discovery Today*, vol. 11, nos. 1–2, pp. 51–57, 2006, https://doi.org/10.1016/S1359-6446(05)03687-1.

[18]J. S. Kutter, M. I. Spronken, P. L. Fraaij, R. A. M. Fouchier, and S. Herfst, "Transmission routes of respiratory viruses among humans," *Curr. Opin. Virol.*, vol. 28, pp. 142–151, Feb. 2018, https://doi.org/10.1016/j.coviro.2018.01.001.

[19]N. Pica and N. M. Bouvier, "Environmental factors affecting the transmission of respiratory viruses," *Curr. Opin. Virol.*, vol. 2, no. 1, pp. 90–95, Feb. 2012, https://doi.org/10.1016/j.coviro.2011.12.003.

[20]K. Randall, E. T. Ewing, L. C. Marr, J. L. Jimenez, and L. Bourouiba, "How did we get here: What are droplets and aerosols and how far do they go? A historical perspective on the transmission of respiratory infectious diseases," *Interface Focus*, vol. 11, no. 6, art. 20210049, 2021, https://doi.org/10.1098/rsfs.2021.0049.

[21]F. Bianco, P. Incollingo, U. Grossi, and G. Gallo, "Preventing transmission among operating room staff during COVID-19 pandemic: The role of the aerosol box and other personal protective equipment," *Updates Surg.*, vol. 72, pp. 907–910, May 2020, https://doi.org/10.1007/s13304-020-00818-2.

[22]S. D. Judson and V. J. Munster, "Nosocomial transmission of emerging viruses via aerosol-generating medical procedures," *Viruses*, vol. 11, no. 10, art. 940, 2019, https://doi.org/10.3390/v11100940.

[23]M. J. Seymour, A. Alani, A. Manning, and J. Jiang, "CFD based airflow modelling to investigate the effectiveness of control methods intended to prevent the transmission of airborne organisms," in *Proc. 7th Int. Conf. Air Dist. Rooms*, Reading, United Kingdom, Jul. 9–12, 2000, vol. 1, pp. 77–82, https://www.aivc.org/sites/default/files/airbase_13188.pdf.

[24]M. Januszewski and M. Kostur, "Sailfish: A flexible multi-GPU implementation of the lattice Boltzmann method," *Comp. Phys. Commun.*, vol. 185, no. 9, pp. 2350–2368, Sep. 2014, https://doi.org/10.1016/j.cpc.2014.04.018.
[25]M. Geier, M. Schönherr, A. Pasquali, and M. Krafczyk, "The cumulant lattice Boltzmann equation in three dimensions: Theory and validation," *Comp. Math. Appl.*, vol. 70, no. 4, pp. 507–547, Aug. 2015, https://doi.org/10.1016/j.camwa.2015.05.001.
[26]X. Wang, C. Shu, J. Wu, and L. M. Yang, "An efficient boundary condition-implemented immersed boundary-lattice Boltzmann method for simulation of 3D incompressible viscous flows," *Comp. Fluids*, vol. 100, no. 1, pp. 165–175, Sep. 2014, https://doi.org/10.1016/j.compfluid.2014.05.014.
[27]L. Ding and A. C. K. Lai, "An efficient lattice Boltzmann model for indoor airflow and particle transport," *J. Aerosol Sci.*, vol. 63, pp. 10–24, Sep. 2013, https://doi.org/10.1016/j.jaerosci.2013.04.004.
[28]S. Sadrizadeh, A. Aganovic, A. Bogdan, C. Wang, A. Afshari, et al., "A systematic review of operating room ventilation," *J. Building Eng.*, vol. 40, art. 102693, 2021, https://doi.org/10.1016/j.jobe.2021.102693.
[29]P. Bischoff, N .Z. Kubilay, B. Allegranzi, M. Egger, and P. Gastmeier, "Effect of laminar airflow ventilation on surgical site infections: A systematic review and meta-analysis," *Lancet Infect. Dis.*, vol. 17, no. 5, pp. 553–561, 2017, https://doi.org/10.1016/S1473-3099(17)30059-2.
[30]W. Whyte and B. H. Shaw, "The effect of obstructions and thermals in laminar-flow systems," *Epidemiol. Infect.*, vol. 72, no. 3, pp. 415–423, 1974, https://doi.org/10.1017/S0022172400023652.
[31]A. Aganovic, G. Cao, L. I. Stenstad, and J. G. Skogås, "An experimental study on the effects of positioning medical equipment on contaminant exposure of a patient in an operating room with unidirectional downflow," *Building Environ.*, vol. 165, art. 106096, 2019, https://doi.org/10.1016/j.buildenv.2019.04.032.
[32]V. Hofer, A. Hartmann, H. Rotheudt, B. Zielke, and M. Kriegel, "Disturbance of a laminar air flow caused by differently shaped surgical lights," *Int. J. Ventilation*, vol. 31, pp. 1–7, 2020, https://doi.org/10.1080/14733315.2020.1861774.
[33]H. Brohus, K. D. Balling, and D. Jeppesen, "Influence of movements on contaminant transport in an operating room," *Indoor Air*, vol. 16, no. 5, pp. 356–372, Oct. 2006, https://doi.org/10.1111/j.1600-0668.2006.00454.x.
[34]COMSOL Inc., "Platform Product: COMSOL MULTIPHYSICS®," comsol.com. https://www.comsol.com/comsol-multiphysics (accessed Nov. 1, 2021).
[35]T. Dinan and D. Wylie, "Expected costs of damage from hurricane winds and storm-related flooding," Congressional Budget Office, Washington, DC, United States, Apr. 2019. https://www.cbo.gov/publication/55019#section4.
[36]T. Knutson, "Global warming and hurricanes: An overview of current research results." GFDL.com. https://www.gfdl.noaa.gov/global-warming-and-hurricanes/ (accessed Nov. 1, 2021).
[37]Federal Emergency Management Agency, "Hazus," fema.gov. fema.gov/flood-maps/products-tools/hazus (accessed Nov. 1, 2021).
[38]W. C. Skamarock, J. B. Klemp, J. Dudhia, D. O. Gill, Z. Liu, et al., "A description of the Advanced Research WRF model version 4," National Center for Atmospheric Research, Boulder, CO, United States, NCAR/TN-556+STR, Mar. 2019. https://opensky.ucar.edu/islandora/object/technotes%3A576.
[39]R. B. Alley, K. A. Emanuel, and F. Zhang, "Advances in weather prediction," *Science*, vol. 363, no. 6425, pp. 342–344, https://doi.org/10.1126/science.aav7274.
[40]H. E. Willoughby, D. P. Jorgensen, R. A. Black, and S. L. Rosenthal, "Project STORMFURY, A Scientific Chronicle, 1962–1983," *Bull. Amer. Meteor. Soc.*, vol. 66, pp. 505–514, 1985, https://doi.org/10.1175/1520-0477(1985)066<0505:PSASC>2.0.CO;2.
[41]K. Klima, M. G. Morgan, I. Grossmann, and K. Emanuel, "Does it make sense to modify tropical cyclones? A decision-analytic assessment," *Environ. Sci. Technol.*, vol. 45, no. 10, pp. 4242–4248, Apr. 2011, https://doi.org/10.1021/es104336u.
[42]M. Z. Jacobson, C. L. Archer, and W. Kempton, "Taming hurricanes with arrays of offshore wind turbines," *Nature Climate Change*, vol. 4, pp. 195–200, Feb. 2014, https://doi.org/10.1038/nclimate2120.
[43]S. A. Keote, D. Kumar, and R. Singh, "Construction of low rise buildings in cyclone prone areas and modification of cyclone," *J. Energ. Pow. Sources*, vol. 2, no. 7, pp. 247–252, Jul. 2015.
[44]K. Emanuel, "Thermodynamic control of hurricane intensity," *Nature*, vol. 401, pp. 665–669, Oct. 1999, https://doi.org/10.1038/44326.
[45]A. White, K. Björkman, E. Grabowski, R. Letelier, S. Poulos, B. Watkins, and D. Karl, "An open ocean trial of controlled upwelling using wave pump technology," *J. Atmos. Ocean. Technol.*, vol 27, no. 2, pp. 385–396, 2010, https://doi.org/10.1175/2009JTECHO679.1.
[46]J. L. Bevin, R. Berg, and A. Hagen, "Hurricane Michael (AL142018)," National Hurricane Center, University Park, FL, United States, May 2019. https://www.nhc.noaa.gov/data/tcr/AL142018_Michael.pdf.
[47]A. Oschlies, M. Pahlow, A. Yool, and R. J. Matear, "Climate engineering by artificial ocean upwelling: Channelling the sorcerer's apprentice," *Geophys. Res. Lett.*, vol. 37, no. 4, art. L04701, Feb. 2010, https://doi.org/10.1029/2009GL041961.
[48]K. Klima, "Does tropical cyclone modification make sense? A decision analytic perspective," PhD thesis, Carnegie Mellon University, Dec. 2011, https://www.cmu.edu/ceic/assets/docs/publications/phd-dissertations/2012/kelly-klima-phd-thesis-2012.pdf.
[49]C. C. K. Liu and Q. Jin, "Artificial upwelling in regular and random waves," *Ocean Eng.*, vol. 22, no. 4, pp. 337–350, 1995, https://doi.org/10.1016/0029-8018(94)00019-4.
[50]P. W. Kithil, "Comments on 'An open ocean trial of controlled upwelling using wave pump technology,'" *J. Atmos. Oceanic Tech.*, vol. 28, no. 6, pp. 847–849, 2011, https://doi.org/10.1175/2010JTECHO778.1.
[51]National Buoy Data Center. "Station 42039 (LLNR 115) – PENSACOLA – 15NM SSE of Pensacola, FL," ndbc.noaa.gov. https://www.ndbc.noaa.gov/station_page.php?station=42039 (accessed Nov. 2, 2021).
[52]Argo. "Argo float data and metadata from Global Data Assembly Centre (Argo GDAC)," seanoe.org. https://www.seanoe.org/data/00311/42182/ (accessed Nov. 2, 2021).
[53]M. D. Powell and T. A. Reinhold, "Tropical cyclone destructive potential by integrated kinetic energy," *Bull. Amer. Meteorol. Soc.*, vol. 88, no. 4, pp. 513–526, Apr. 2007, https://doi.org/10.1175/BAMS-88-4-513.

Ryan A. Darragh, Research and Exploratory Development Department, Johns Hopkins University Applied Physics Laboratory, Laurel, MD

Ryan A. Darragh is a computational physicist in APL's Mechanical Engineering Systems Analysis and Design Group. He has a BA in physics and mathematics from Kenyon College and a PhD in aerospace engineering sciences from the University of Colorado at Boulder. His current research focuses on combining machine learning and computational fluid dynamics to study mixing and transport of aerosols in indoor environments. Other research interests include turbulence, multiphase flows, and combustion. His email address is ryan.darragh@jhuapl.edu.

Victoria J. Campbell, Research and Exploratory Development Department, Johns Hopkins University Applied Physics Laboratory, Laurel, MD

Victoria J. Campbell is a mechanical engineer in APL's Mechanical Engineering Systems Analysis and Design Group. She has a BS and an MEng in mechanical engineering from Cornell University. Her work has ranged from detailed mechanical design and drawings for electronics packaging to finite element analysis for high-speed impact. Other research interests include climate change and its impact on Earth systems, renewable energy, and disasters, in association with geoengineering concepts. Her email address is victoria.campbell@jhuapl.edu.

Nathaniel S. "Pete" Winstead, Force Projection Sector, Johns Hopkins University Applied Physics Laboratory, Laurel, MD

Pete Winstead is a meteorologist in APL's Oceanic, Atmospheric and Remote Sensing Sciences Group. He received a BS in mathematics from Duke University and an MS and a PhD in meteorology from the Pennsylvania State University. He is an expert in modeling the Earth system with experience in a wide range of atmosphere and ocean models, including weather research and forecasting, regional ocean modeling, atmosphere, and ocean large-eddy simulations. His current research focuses on the development of a robust Earth systems modeling capability for simulating the atmosphere/ocean system at scales ranging from global to turbulence to support environmental and climate analysis at APL. His email address is nathaniel.winstead@jhuapl.edu.

Raymond K. Lennon, Research and Exploratory Development Department, Johns Hopkins University Applied Physics Laboratory, Laurel, MD

Raymond K. Lennon is a college intern in APL's Mechanical Engineering Systems Analysis and Design Group. He is pursuing a bachelor's degree in mechanical engineering at Duke University as an incoming senior. He specializes in computational physics simulation and modeling and currently works on problems involving fluid dynamics, visualization, and computational design optimization. He has worked at APL since 2017, both as an ASPIRE intern and a college intern. His email address is ray.lennon@jhuapl.edu.

Christopher D. Stiles, Research and Exploratory Development Department, Johns Hopkins University Applied Physics Laboratory, Laurel, MD

Christopher D. Stiles is a computational physicist and supervisor of the Multiscale Mathematical Modeling Section in APL's Research and Exploratory Development Department. He holds a BS in mathematics and physics and a PhD in nanoscale science and engineering, both from the State University of New York at Albany. Christopher specializes in computational approaches of materials science to model real-world systems—developing, using, and advising on the use of cutting-edge computational methods. His email address is christopher.stiles@jhuapl.edu.